Send Orders for Reprints to reprints@benthamscience.net

434 *Current Nanoscience,* **2013**, *9*, 434-441

Nanoparticles of Lyotropic Liquid Crystals: A Novel Strategy for the Topical Delivery of a Chlorin Derivative for Photodynamic Therapy of Skin Cancer

Raquel Petrilli[1], Fabíola S.G. Praça[1], Aline Regina H. Carollo[1], Wanessa S.G. Medina[1], Kleber Thiago de Oliveira[2], Márcia C.A. Fantini[3], Maria da Graça P.M.S. Neves[4], José A.S. Cavaleiro[4], Osvaldo A. Serra[5], Yassuko Iamamoto[5] and Maria Vitória L.B. Bentley*[1]

[1]*Faculdade de Ciências Farmacêuticas de Ribeirão Preto, Universidade de São Paulo, Av. do Café, s/n, CEP 14040-903, Ribeirão Preto, SP, Brazil;* [2]*Departamento de Química, Universidade Federal de São Carlos, Brazil;* [3]*Instituto de Física, Universidade de São Paulo, Brazil;* [4]*Department of Chemistry and QOPNA, University of Aveiro, Portugal;* [5]*Departamento de Química, Faculdade de Filosofia, Ciências e Letras de Ribeirão Preto, Universidade de São Paulo, Brazil*

Abstract: Nanoparticles of lyotropic liquid crystals loaded with a new photosensitizer (a chlorin derivative) were developed for use in photodynamic therapy (PDT). These systems were characterized by spectrofluorimetric, dynamic light scattering, and small angle X-ray diffraction (SAXRD) analyses. *In vitro* and *in vivo* penetration studies in animal models were performed using animal model membranes. The systems had a particle size of 161 ± 4 nm and a polydispersity index of 0.175 ± 0.027. Furthermore, SAXRD studies demonstrated that the preparations remained in the liquid crystalline phase type hexagonal after drug loading. The encapsulation rate was higher than 50%, and cell viability studies revealed that the nanodispersion is not harmful for L929 skin cells. *In vitro* and *in vivo* penetration studies confirmed that the nanodispersion of hexagonal phase enabled a higher drug skin uptake compared to the control. Additionally, a fluorescence microscopy study demonstrated a higher biodistribution of the chlorin derivative in the skin layers of hairless mice compared to the control. Taken together, the results show the potential of this nanodispersion for the delivery of the photosensitizer into the skin, which is a crucial condition for successful topical PDT.

Keywords: Photodynamic Therapy, skin delivery, chlorin, nanoparticles, liquid crystal.

INTRODUCTION

Photodynamic therapy (PDT) is an emerging technology for the important therapeutic options concerning the management of neoplasic and non-neoplasic diseases. PDT is based on the administration of a photosensitizing drug (PS) and its selective retention in the malignant tissue [1]. PS can be administered systemically, locally, or topically [2]. The last step in PDT is the activation of a PS by application of light at a wavelength that matches the PS absorption features [3]. Photophysical reactions take place in this situation, which in turn results in cell death due to the production of free radicals and/or reactive oxygen species, especially singlet oxygen ($^1O_2$) [4].

The major limitation of topical PDT is the poor penetration of PSs through biological barriers, like the normal skin. A series of PSs are under study in PDT experiments; however, most of them are relatively hydrophobic and have low capacity of accumulation in the target tissue. In this way, designed delivery systems is a tool in pharmaceutical field [5], and recently, studies have focused on the development of different strategies to overcome these difficulties, including the use of nanocarriers [6], liposomes [7], ethosomes [8], invasomes [9], and magnetic nanoparticles [10], among others.

In addition to the delivery system approach, several research groups have been dedicated to the study of lyotropic liquid crystals, which combine the properties of crystalline solid with those of an isotropic liquid [11]. Due to their ideal structural properties, they have shown excellent results as vehicles for a variety of drugs, once they can accommodate the drug within both their aqueous and lipid domains [12, 13].

*Address correspondence to this author at the Faculdade de Ciências Farmacêuticas de Ribeirão Preto, Universidade de São Paulo, Av. do Café, s/n, CEP 14040-903, Ribeirão Preto, SP, Brazil; Tel/Fax: + 55 16 36024301; E-mail: vbentley@usp.br

A reverse hexagonal phase of liquid crystal containing monoolein has been shown to increase topical drug delivery [14, 15]. Carr *et al.* [16] have studied these systems and concluded that some components of Myverol (commercial monoolein) could enhance the passive penetration of nicotine into the human stratum corneum, thus demonstrating the effectiveness of this vehicle for transdermal drug delivery. Liquid crystalline phases containing monoolein increased the skin delivery of cyclosporine A, both as a bulk phase [17] and as a nanodispersed formulation [14]. Further studies have shown that therapy with topical vitamin K could be improved by using monoolein-based systems [15]; and, recently, the skin delivery of siRNA was achieved by nanodispersion of reverse hexagonal phase [18].

Despite the potential of liquid crystalline systems to deliver drugs into the skin, few studies have used this type of carrier for PDT to deliver PS topically. In this aspect, we propose in the present work a delivery system for PDT based on a nanodispersion of liquid crystalline phase, aiming at increasing the delivery of chlorin derivatives into the skin. To this end, nanoparticles of reverse hexagonal phase loaded with this PS were developed and their *in vitro* and *in vivo* topical applications were evaluated. To our knowledge, this is the first report of a biological and pharmaceutical application of 2^1-methoxycarbonyl-13,17-bis[2-(methoxycarbonyl)ethyl]-2,7,12,18-tetramethyl-8-vinyl-2,2^1,2^2,2^3-tetrahydrobenzo[b]porphyrin-22-carboxylic acid and 2^1-methoxycarbonyl-8,12- bis[2-(methoxycarbonyl)ethyl]-2,7,13,17-tetramethyl-18-vinyl-2,2^1,2^2,2^3 tetrahydrobenzo[b]porphyrin-22-carboxylic acid, a mixture of chlorin derivatives.

MATERIAL AND METHODS

Materials

Chlorin derivatives (Fig. **1**) were synthesized according to a procedure described before [19] and were used as a diastereomeric mixture. Briefly, these lipophilic compounds were obtained through a Diels-Alder reaction; the reaction in ring A of protoporphyrin IX

1875-6786/13 $58.00+.00

dimethyl ester (PpIXDME) yielded chlorin A, whilst the reaction in ring B of PpIXDME yielded chlorin B. Since these chlorin derivatives are very similar in terms of polarity, we decided to use them as a diastereomeric mixture (chlorin A + chlorin B) in all studies, and only one purification step was accomplished, in order to remove by-products. The mixture chlorin A + chlorin B is referred as PS in the following sections.

Monoolein (Myverol 18-99®) (MO) was purchased from Quest International (USA); oleic acid (OA) and octanol were obtained from Sigma-Aldrich (Sao Paulo, Brazil); methanol was acquired from Bdick & Jackson (B & J ACS / HPLC Certified Solvent); poloxamer 407 a polyoxyethylene (101 units)–polyoxypropylene (56 units) copolymer, was supplied from BASF (Florham Park, New Jersey); polyethylene glycol 300 (Carbowax 300) was supplied by Synth (Diadema, Brazil). Sephadex LH20 was provided by GE Healthcare. Water was purified using a Millipore milli-Q water system (Millipore Corporation).

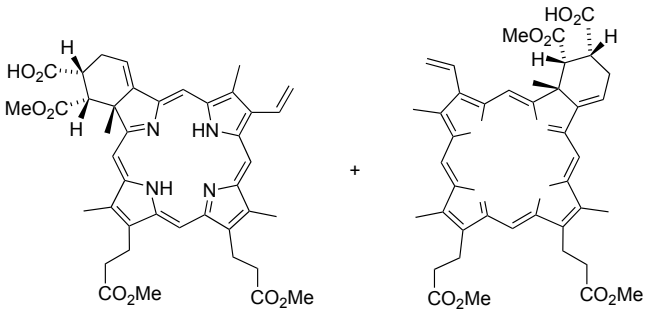

Fig. (1). Chemical structures of the studied chlorins: (**a**) Chlorin **A** and (**b**) Chlorin **B**

Spectrofluorometric Assay

The PS was assayed by spectrofluorometry using a Fluorolog 3 Triax 550 (Edson, NJ, USA) apparatus, working at 400 and 670 nm of excitation (λ_{exc}) and emission (λ_{em}), respectively, using a bandwidth of 1 nm [19, 20]. An analytical method was developed and evaluated with respect to linearity, precision, accuracy, limits of detection (LOD), and lower limit of quantification (LLOQ). A linear calibration curve was performed using standards solutions obtained from serial dilutions of a methanolic solution of chlorin (25 mg/mL). The LOD was the basis of signal-to-noise ratios (S/N) of 3:1, and the LLOQ was considered as the quantified minimum concentration of chlorin with acceptable linearity $r \geq 0.99$ (S/N 10:1). The stability of the samples containing the PS was also assessed. Thus, PS solutions of different concentrations were solubilized in either methanol or phosphate buffer pH 7.2 containing polyssorbate 80 at 2%, and evaluated at 12 and 120 h after preparation by spectrofluorometry. Furthermore, it was necessary to evaluate whether porcine ear skin would affect the PS fluorescence spectrum. So, the outer skin of pig ears was removed from recently killed animals with the aid of a forceps and a scalpel, followed by removal of the fatty tissue that remained in the skin. Skin sections were dermatomed to 500 μm (Dermaton, Nouvag, Switzerland). An area of about 1.44 cm^2 skin was measured and then fragmented into small pieces. The fragments were added to drug methanolic solution, mixed in a Turrax instrument for 1 min, and then sonicated using an ultrasonic bath for 24 min. The samples were centrifuged for 10 min at 1901 *g*, and the supernatant was analyzed by spectrofluorometry at the same conditions as those employed for the PS method.

Preparation of the Formulations

The hexagonal liquid crystalline phase nanodispersion was prepared using a previously published method [14]. Briefly, the PS (1 mg) was dissolved in 0.3 g of the lipid phase (OA:MO mixture at a 2:8 ratio) and 2.7 g of the citrate buffer (pH 6) containing 1.5% Poloxamer 407. The system was allowed to equilibrate at room temperature for 24 h and was then vortex-mixed for 2 min and sonicated in ice-bath at 10 kHz for 2 min. The obtained mixture was centrifuged at 1901 *g* for 10 min and then filtered using a 0.8 μm porous membrane. The control formulation consisted of a PS in polyethylene glycol (PEG) (MW 300, 0.3 mg/g). The control was obtained by vortex-mixing the PS in this solvent for 5 min at 3.000 rpm, followed by centrifugation at 1901 *g* for 10 min. The concentration of PS in both formulations (control and nanodispersion) was assessed spectrofluorometrically after each preparation.

Physicochemical Characterization of the Nanodispersion

a) Polarized Light Microscopy

The texture of the reverse hexagonal liquid crystalline phase was observed under an optical microscope Axioplan 2 (Zeiss, Germany) equipped with a polarizing filter and coupled to a digital camera Axiocan HRc (Zeiss, Germany), which is equipped with a video system and automatic image acquisition. The observations were accomplished at 25 ºC (average room temperature) and 37 ºC (average body temperature) by using a hotplate model THMSG 600 (Link, England) coupled to the polarized light microscope.

b) Turbidimetric Analysis

The samples were analyzed at 25 ºC, and the values of apparent absorbance at 410 nm were obtained on a spectrophotometer (FentoScan, Brazil). Non-loaded and PS-loaded hexagonal liquid crystalline phase nanodispersions were diluted in citrate buffer, pH 6.0 (1:50), and then analyzed for 72 h. The diluted samples were packed and stored in a quartz cuvette with a 0.5 cm light path to prevent disruption of the system during reading caused by sample manipulation. The experiments were performed in triplicate.

c) Dynamic Light Scattering

The particle size, polydispersity index (Pdl) and zeta potential of the hexagonal liquid crystalline phase nanodispersion were analyzed by the light scattering method (DLS) in a Zetasizer 3000 HSA apparatus (Malvern Instruments). Particle size/ Pdl were determined using 10mW HeNe laser operating at 633 nm with an incidence detection angle of 173º, at 25 °C and zeta potential was determined by the standard capillary electrophoresis cell. Measurements of the position within the cuvette were automatically determined by the software. The analyzed samples (n=3) were: (i) Nanodispersions without PS, processed by centrifugation at 1901 *g* for 10 min and filtration using a 0.8 μm porous membrane; (ii) Nanodispersions containing PS and processed by centrifugation at 1901 *g* for 10 min; (iii) Nanodispersions containing PS and processed by filtration using a 3 μm porous membrane; (iv) Nanodispersion containing PS chlorin and processed in the same as (i).

d) Small Angle X-ray Diffraction (SAXRD)

To characterize the liquid crystalline structure of the dispersed particles, small-angle synchrotron radiation X-ray diffraction (SAXRD) measurements were performed at the Brazilian Synchrotron Light Laboratory (LNLS) in Campinas, SP, Brazil, using the D12A-SAXS beam line. The selected wavelength was 0.1488 nm. Scattered intensities curves were recorded using a two-dimensional, position-sensitive MARCCD detector (Rayonix LLC, Evanston, IL, USA) located at 803.3 mm from the sample, and an ionization detector was responsible for monitoring the intensity of the incident beam. The measurements were carried out with an exposure time of 5 min, at 25 ºC. The data were corrected by detector homogeneity, incident beam intensity, sample absorption, and dark noise and blank (buffer solution containing Poloxamer) subtraction. Non-loaded and PS-loaded hexagonal phase nanodipersions were analyzed.

e) Analysis of the Encapsulation Degree by Gel Chromatography

Non-encapsulated PS was removed from the hexagonal liquid crystalline phase nanodispersion by size exclusion chromatography using a Sephadex LH-20 column (3.5 cm diameter, measuring 17 cm after packaging of the column). The samples (500 µL) were placed on the Sephadex column and eluted using purified water as the mobile phase. The eluted fractions were monitored by turbidity measurements at 410 nm using a FEMTO 800XI spectrophotometer (Sao Paulo, Brazil). Around 30 fractions were collected; 1 mL aliquots of each fraction were lyophilized, to remove water. After the lyophilization process, the samples were solubilized in 3 mL of methanol and assayed for the PS by spectrofluorimetry (λ_{exc}= 400 nm, λ_{em}= 670 nm) [21]. The concentration applied was considered as 100% and the concentration obtained after elution in the fractions corresponding to the encapsulated PS was compared with this value, resulting in the encapsulation degree of the samples. The experiment was conducted in triplicates, providing the error value.

Cell Viability

a) Cell Culture and Treatment

L929 cells were grown in 150 cm² tissue culture flasks in DMEM cell culture medium supplemented with 1% (v/v) of an antibiotic solution containing, 10000 UI of penicillin, 10 mg streptomycin and 25 µg of amphotericin B per mL and 10.0% (v/v) heat-inactivated FBS at 37°C under 5% CO_2. The cytotoxicity of the nanodispersion of hexagonal phase was evaluated comparing the viability of the cells for: (i) nanodispersion without the PS; (ii) nanodispersion containing the PS; (iii) aqueous solution of the PS at the same concentration of group (ii), (iv) PBS and (v) Triton X-100 0.5%.

b) MTT Assay

Tetrazolium salts such as MTT are common tools applied for analysis of cytotoxicity of drugs in a variety of cell cultures [22]. This method is commonly used and is based on the reduction of the MTT tetrazolium salt (2-(4,5-dimethyl-2-thiazolyl)-3,5-diphenyl-2H-tetrazolium bromide) that occurs when viable cells metabolize it in order to produce an purple formazan [22]. The cell viability induced by the PS was evaluated by the spectrophotometric MTT assay. For this experiment, $5x10^4$ cells/well were seeded in 96-well plates and incubated for 24 h at 37°C in atmosphere of 95% air and 5% CO_2. After this, 20 µL of the formulations (i) to (iii) diluted in PBS (1:50) were added to the culture plates for 24 h. Then, cells were washed with saline solution twice and serum-free culture medium in the absence of phenol red was added to the cell plates. A MTT solution of 5 mg/mL was added and cells were incubated for 4 h. After this procedure, the medium containing the MTT reagent was discarded and the formazan crystals were solubilized in 200 µL of DMSO and 25 µL of glycine buffer 0.2 mol/L pH 10.2. The spectrometric method was applied for the quantifications by measuring the absorbance values at 570 nm with a microplate reader (Quant™, BioTek Instruments Inc., USA). The cellular viability was calculated as the percentage of viable cells compared to the control group.

Skin Penetration Studies

a) In vitro Skin Retention Studies

Skin from the outer portion of freshly excised porcine ears was dissected with the aid of a scalpel and then dermatomed (~500 µm). The skin was stored at -20°C and used within one month. For the experiments, the skin sections were placed on a Franz cell diffusion (diffusion area of 0.79 cm^2) with stratum corneum (SC) facing the donor compartment, which was filled with 100 µL of hexagonal phase nanodipersions (Fig. **2E**) or PEG 0.3 mg/g used as control formulation (n= 6 for each preparation), which causes dehydratation and membrane fusion, leading to an asymmetry of lipid packing and thus acting as an absorption promoter [23]. The receiver compartment was filled with 3 mL of 100 mM phosphate buffer (pH 7.2 ± 0.2) containing 2% of polyssorbate 80, to improve PS solubility in the receptor medium. The system was kept at 37 °C using a thermostatic water bath. After the time of experiment (4, 8, or 12 h), the system was turned off, the skin surfaces were removed, gently washed with distilled water, and the excess water was removed with a piece of cotton. PS penetration into the skin layers was assessed as described before [17]. In order to separate SC and epidermis plus dermis (E+D), the tape stripping process was applied using 15 tapes (Durex® 3M), considering that the first one was discarded and the following strips were dipped in a Falcon tube containing 5 mL of methanol. These were vortex-mixed and bath-sonicated for 2 and 30 min, respectively. The samples were filtered using a 0.45 µm porous membrane, providing the values of PS retained in the SC. Next, the remaining skin tissue was cut into small pieces and immersed into 5 mL methanol, vortex-mixed for 1 min, bath-sonicated for 30 min, and then filtered in the same way as mentioned above (E+D). Both methanolic samples were assessed by spectrofluorometry (λ_{exc}= 400 nm, λ_{em}= 670 nm), in order to quantify the PS concentration. The recovery rate imposed by the method had been previously tested using small pieces of porcine ear skin measuring 1.44 cm^2, to which 30 µL PS methanolic solution at 12.5 µg/mL were added. The same procedure was applied in the absence of the skin, and the PS concentrations were assessed and compared by spectrofluorometry.

b) In vivo Skin Retention Studies

These studies were conducted according to the methodology standardized by De Rosa *et al.* (2003) [24] and Lopes *et al.* (2006) [17]. The experiment employed hairless mice (male/female six to eight weeks old) strain HRS/J, obtained from Jackson Laboratories (Bar Harbor, ME, USA), housed at controlled temperature (24-26°C) and daily 12:12h light/dark cycles with food and water *ad libitum*. The *in vivo* protocol was approved by the University of São Paulo Animal Committee on Care and Handling (Authorization number 10.1.160.53.0). Animals were separated into 2 groups (6 animals per group), namely the PEG group and the hexagonal liquid crystalline phase nanodispersion group. The formulations were applied on a limited area (2 cm²) of the back of healthy hairless mice using 150 µL of the formulations with the aid of a brush. After 8 h, the mice were euthanized by rising carbon dioxide vapor, and the application area in the skin was dissected for PS quantification. The PS present in the skin was then extracted as described for *in vitro* skin retention and assessed by spectrofluorometry (λ_{exc}= 400 nm, λ_{em}= 670 nm).

c) Fluorescence Microscopy

Cross sections of skin samples obtained at the end of the *in vivo* experiments were embedded in a Tissue-TeK® matrix (O.C.T compound) and frozen at -17 °C, for visualization of the skin penetration of PS by fluorescence microscopy. Then, the samples were cut into vertical slices of 30 µm thickness with the aid of a cryostat (HM550, Microm, Heidelberg, Germany) and observed under a fluorescence microscope (AxiosKop 2 plus, Carl Zeiss, Germany) operating with 395 and 440 nm band-pass excitation and emission filter, respectively. The obtained images were recorded using a digital camera device (AxioCam HR, Carl Zeiss, Germany).

Statistical Analyses

In vitro and *in vivo* studies were analyzed using non-parametric tests (Mann Whitney Test). A 0.05 level of probability was taken as the level of significance ($p<0.05$).

RESULTS AND DISCUSSION

Quantitative Analysis

Analytical methodology Good linearity was obtained in the concentration range from 0.08 to 0.4 µg/mL (r= 0.99). LOD and LLOQ were determined as 6 and 12 ng/mL, respectively. Addition-

ally, intra and inter-day precision assays demonstrated that variation coefficients were lower than 5%. Accuracy was higher than 94% in the inter-day assay. Both methanolic and phosphate buffer solutions of PS demonstrated adequate stability, showing that solvents do not significantly change the stability of the analyte during the whole experiment period. Additionally, porcine ear skin did not affect the PS fluorescence spectrum.

Physicochemical Characterization of the Nanodispersion

a) Polarized Light Microscopy

Polarized light microscopy of liquid crystalline hexagonal phases with or without PS revealed a fan-like texture, typical of hexagonal phase systems (Fig. **2A**, **2C**, and **2D**), indicating that the presence of PS and Poloxamer did not change the characteristics of the systems. In addition, it was observed that the increase in temperature from 25 ºC to 37 ºC did not change the hexagonal liquid crystalline structure of the system, which is characterized by irregular striations, as shown in the Fig. (**2B** and **2D)**, respectively. After dispersion of the hexagonal phase by sonication, the system resulted in a milky and low-viscosity formulation (Fig. **2E**), as already reported previously [15]. The stability of the system was maintained up to 30 days of sample preparation.

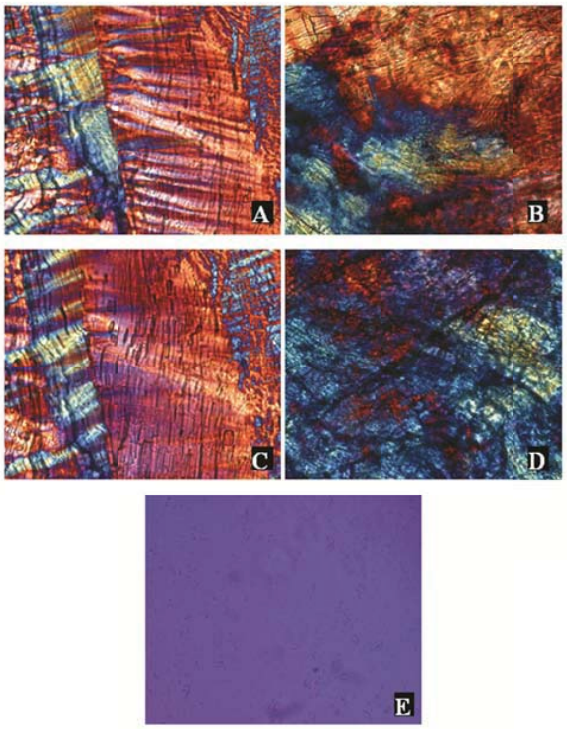

Fig. (2). Characterization of the liquid crystalline phase by polarized light microscopy at 32X: (**A**) Hexagonal phase gel composed of MO/AO/water at a 8:2:90 ratio at 25˚C, after 24 h of preparation; (**B**) Hexagonal phase gel shown in A at 37˚C after 24 h of preparation; (**C**) and (**D**) are the same hexagonal phase containing the drug at 25˚C and 37˚C, respectively; (**E**) Dispersion obtained after sonication of the hexagonal phase composed of MO/AO/water at a 8:2:90 ratio.

b) Turbidimetric Analysis

Turbidimetry can be used to characterize the particle size distribution and verify the stability of colloidal suspensions.

Fig. (**3**) shows the stability of the hexagonal liquid crystalline phase nanodispersion with or without the PS, during a period of 72 h. The wavelength of 410 nm was chosen to verify the presence of nanodispersions in the sample, which is characterized by the turbidity of the sample. The presence of the PS in the nanodispersion leads to less variation in the absorbance at 410 nm when compared to the control, which may indicate that the PS increases the system stability due to the formation of a more rigid structure.

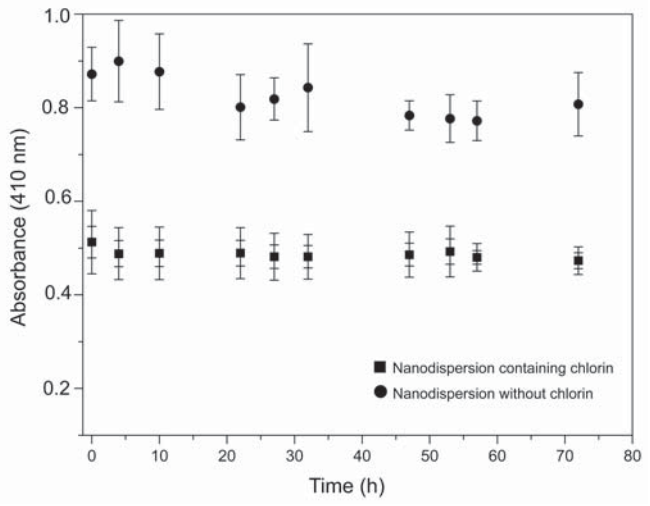

Fig. (3). Turbidimetry (410 nm) results for nanodispersions with or without PS. The bars correspond to the mean ± SD of the results in n = 3 experiments.

c) Dynamic Light Scattering

Table **1** summarizes the results for particle size of hexagonal liquid crystalline phase nanodispersions obtained by different processes. Among the factors that can affect the particle size, we can mention the manufacturing process (sonication) and the components of the formulation. The preparation method consisting of a combination of filtration and centrifugation (groups 1 and 4) resulted in smaller particle size, about 160 nm. The filtration process alone did not resulted in appropriate particle size (group 3), while the centrifugation process (group 2) gave rise to slightly larger particles compared to groups 1 and 4. There were no significant differences between groups 1 and 4 in terms of mean particle size and polidispersity, so the addition of PS did not affect particle size when the hexagonal liquid crystalline phase nanodispersion was submitted to centrifugation and filtration, as already described. According to Lopes *et al.* (2006), the sonication process in the case of the hexagonal phase consisting of MO-water-poloxamer leads to the formation of hexagonal phase nanodispersion, with particles with diameter around 200 nm. The systems obtained herein displayed a profile similar to those obtained with incorporation of other drugs [14, 15]. Considering the role of excipients on the particle size profile, the poloxamer 407 copolymer was applied in the hexagonal liquid crystalline phase nanodispersion, and its concentration may alter the particle size, as already demonstrated by others [25, 26]. The range of particle size obtained in this study is in agreement with previous studies of Nakano *et al.* 2001 [26], where different concentrations of poloxamer in MO provided particle sizes ranging from 160 to 270 nm. Zeta potential was -12.47 (± 0.15) mV and -14.37 (±0.50) mV for nanodispersions without and with the PS, respectively ($p \leq 0.01$, Student T Test).

d) Small Angle X-ray Diffraction (SAXRD)

The SAXRD profile of the liquid crystalline phases revealed three diffraction peaks (ratio 1 / 1, √ 3, √ 4), consistent with the hexagonal phase structure [27] and agreeing with previous works [14]. The lattice parameter (*a*) and the full width at half maximum

Table 1. Particle Size and Distribution as Determined by the Dynamic Light Scattering Method

Sample	Particle size* (nm)	Polydispersity*
Group 1 - Nanodispersion without PS (centrifugation and filtration process)	160 ± 5	0.177 ± 0.004
Group 2 - Nanodispersion containing PS (centrifugation process)	167.5 ± 1.5	0.213 ± 0.011
Group 3 - Nanodispersion containing PS (filtration at 3μm)	192 ± 3	0.340 ± 0.021
Group 4 - Nanodispersion containing PS (centrifugation and filtration at 0.8 μm)	161 ± 4	0.175 ± 0.027

* Mean ± SD of the results in three replicates experiments are shown.

(FWHM) of the nanodispersions were determined, to investigate the effect of PS addition on the hexagonal structure of the particles, since the delivery systems must accommodate drugs in its internal structure without causing disruption or changes in the liquid crystalline phase [28].

Fig. (**4**) shows that the "*a*" value for the samples containing the drug (a = 5.860 ± 0.004) nm is smaller than that observed in the absence of PS (a = 6.150 ± 0.001) nm. This decrease suggests that the drug is located within the hydrophobic layer of the nanoparticle, which can cause an approximation of the hydrophilic layer due to a more negative membrane curvature, thereby decreasing the "*a*" values [28, 29].

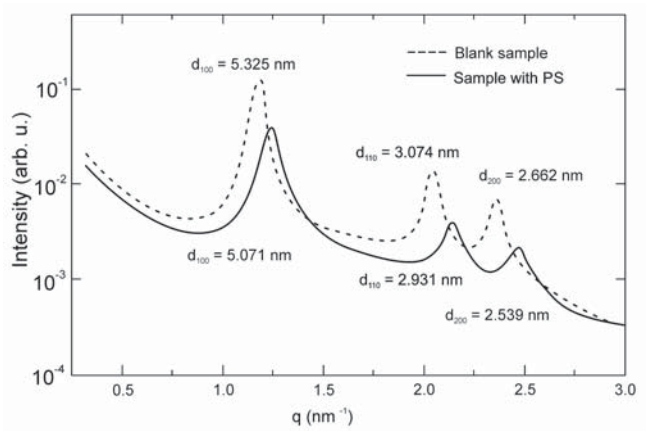

Fig. (4). Diffraction peaks obtained for the blank and nanodispersion (λ=0.1488 nm, exposure time 5 min, 25˚C).

The FWHM values reflect the extension of the disorder caused by the addition of molecules to the liquid crystalline structure. Its increase reflects a less ordered structure, while its reduction indicates a more ordered organization [28]. The FWHM of the sample containing PS (0.098 nm^{-1}) is higher than that of the blank system (0.064 nm^{-1}). Therefore, the PS provoked disorder in the structure, but it did not destroy the periodic micellar arrangement. This is a desirable result, since the release of PS should be more efficient in the ordered hexagonal channels, which must provide a better diffusion path for the PS molecule.

e) Analysis of the Encapsulation Degree by Gel Chromatography

Several methods have been employed to separate the free form of drugs, including ion exchange chromatography, ultrafiltration and size exclusion chromatography [30]. Size exclusion chromatography is the most widely used because of its simplicity, reproducibility, and its applicability to different kinds of preparations. In the present study, the hexagonal liquid crystalline phase nanodispersion containing PS gave rise to eluted fractions containing PS in both the encapsulated and free form. The nanodispersion was eluted from the column with water between fractions 7 and 16. Macroscopically, these fractions were whitish, besides presenting high values of absorbance at 410 nm. When it contained the PS, the nanodispersion was eluted in the same fractions, whereas the non-encapsulated PS was eluted from the column by methanol between fractions 8 and 10. Assay of these fractions by spectrofluorometry showed an encapsulation degree of 52.10% (± 2.82) for PS.

Cell Viability

Studies of cell viability of L929 mice fibroblasts are a great model for evaluating the cytotoxicity of the nanodispersions studied, since a low toxicity is required for a topical formulation [31]. With this purpose, the nanodispersions containing or not the PS were compared to an aqueous solution of the PS and water, aiming a comparison between our studied nanodispersion and a vehicle known by its safety in contact with the skin. The results revealed a cell viability of 102.9% ± 13.0% ($p \geq 0.05$) and 119.7% ± 16.3% ($p \leq 0.05$) for the nanodispersion without and with the PS, respectively, which demonstrates that both do not harm the integrity of the skin cells. These results can be compared to those obtained for groups (iii), (iv) and (v), which have shown cellular viability rates of 67.6% ± 11.9% ($p \leq 0.05$), 102.9% ± 10.2% ($p \geq 0.05$) and 10.1% ± 12.8% ($p \leq 0.05$), respectively. Considering that PBS is not toxic for the skin and the limitation imposed by the method which leads to values statistically different between some groups, the PS encapsulated in the nanodispersion did not present toxicity for the skin, demonstrating that it is safe for photodynamic therapy of skin cancer. Furthermore, the nanodispersions containing or not PS showed cellular viability higher than the drug alone, probably due to the sustained release that such system can provide. Triton X-100 0.5% is known to be a moderate irritant for the skin and it was responsible for the low cell viability values.

Skin Pernetration Studies

a) In vitro Studies

The penetration properties are determined by the OECD Guideline TG 428: Skin Absorption: *in vitro* Method [32], which allows the use of porcine skin for penetration studies. Porcine ear skin is considered an alternative to human skin for *in vitro* penetration studies, because it has histological similarity to human skin tissue, in terms of epidermal thickness and composition, pelage density, epidermal lipid biochemistry, and general morphology. An excel-

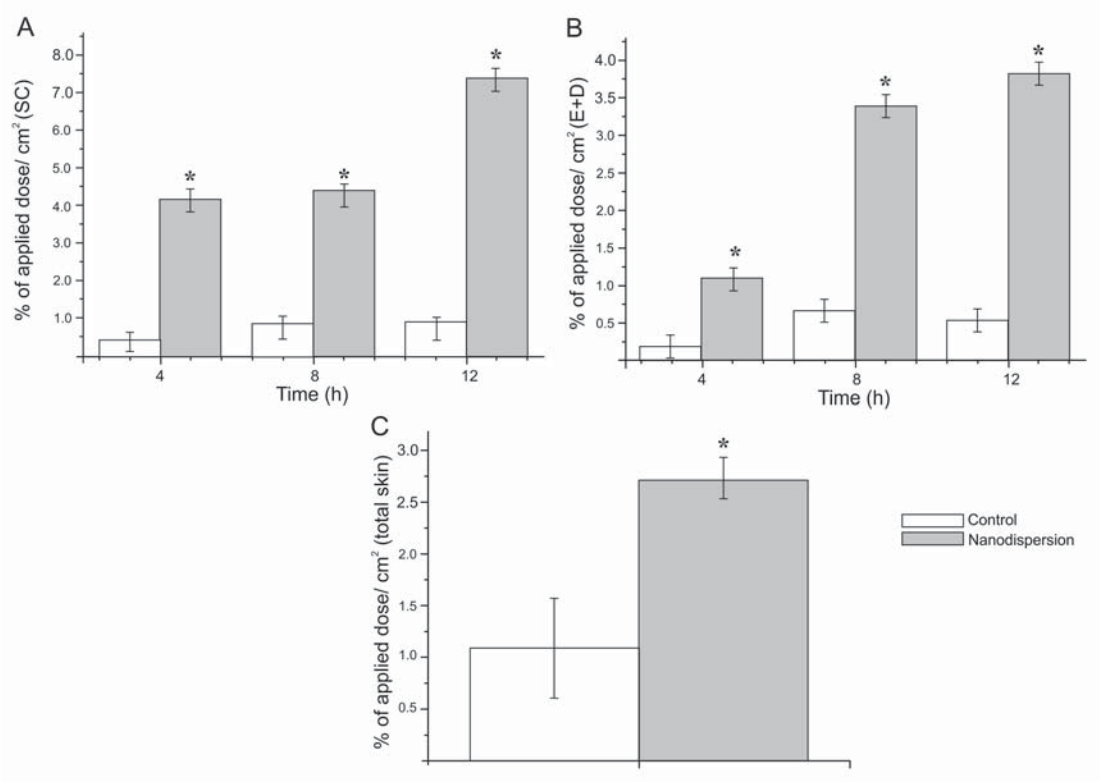

Fig. (5). Skin penetration studies of PS incorporated in hexagonal nanodispersion and control formulation (PEG): *In vitro* PS penetration in SC (**A**) and E+D (**B**) and *in vivo* penetration of PS in total skin (**C**). Results expressed as mean ± SD of the results in six replicate experiments. *significantly increase ($p < 0.01$) compare to control formulation.

lent correlation between permeation data using porcine ear skin *in vitro* and human skin *in vivo* has been demonstrated [33].

Fig. (**5**) presents the results of *in vitro* and *in vivo* skin penetration (SC and E+D and total skin, respectively) of PS in the hexagonal liquid crystalline phase nanodispersion and control formulation. The nanodispersion was able to promote a significantly increase ($p < 0.01$) in the amount of PS retained in the skin at all the studied times (Fig. **5A** and **5B**). PS retention in E + D increased over time; after 4 and 12 h post application, it became about five and seven times greater compared to the control, respectively. This result could be explained by the characteristics of the lipids present in the formulation (MO and OA), since they can affect the integrity of the skin barrier [14, 15, 17, 23]. The use of lipid colloidal dispersions for topical and percutaneous drugs administration of drugs has been studied [34, 35], and some works have described that the composition and particle size of dispersion systems can influence the skin penetration depth of encapsulated drugs [36].

In the present work, we can refer the significant enhancement effect of the hexagonal liquid crystalline phase nanodispersion with respect to PS delivery into the skin layers in both situations, i.e., the penetration enhancement effect of its lipid composition and the increase of the contact area due to the nanosized carrier, which can improve the skin uptake of the PS.

The *in vitro* results of the present research are in accordance with the ones reported by Lopes *et. al.* 2006 and 2007, who demonstrated increased skin retention of the lipophilic cyclosporine A using liquid crystalline nanodispersion systems [14, 15]. This shows that liquid crystalline phases containing MO are promising for application in a variety of treatments that depend on the drug delivery to the viable epidermis. It should be noted that the PS recovery rate from the skin using the extraction method was greater than 94%, which was suitable for spectrofluorometric quantification. PS concentrations were not detected in the receptor phase (phosphate buffer containing 2% polyssorbate 80) by the spectrofluorometric assay used here.

b) In vivo Studies

The *in vivo* skin retention of PS was carried out after 8 h of topical application. The hexagonal liquid crystalline phase nanodispersion significantly improved PS skin penetration compared to control formulation (Fig. **4C**). While the control formulation enabled 1.09 ± 0.48% of applied dose/cm^2 retention in the skin, the nanodispersion developed here was responsible for rates equal to 2.72 ± 0.21% of applied dose/cm^2 ($p<0.05$). This result is similar to that obtained in studies by our research group using cyclosporine A incorporated into this hexagonal phase nanodispersion [17].

Considering the differences in the cutaneous permeation between different model membranes used in the *in vitro* and *in vivo* studies, we can assume that both penetration studies confirm an increase in PS delivery into the skin layers when hexagonal liquid crystalline phase nanodispersion was used as a carrier.

c) Fluorescence Microscopy

When the control formulation composed of PEG and PS was topically applied, the resulting fluorescence was predominantly present in the SC, and a weak fluorescence could be observed in only some regions of the epidermis (Fig. **6B**). Nevertheless, treatment of mouse skin with the hexagonal liquid crystalline phase nanodispersion containing PS resulted in increased fluorescence in the SC, viable epidermis, and even in some regions of the dermis, as seen in Fig. (**6D**). Fig. (**6A**) and (**6C**) correspond to the same skin pieces as those represented in Fig. (**6B**) and (**6D**), respectively, but without the use of fluorescence methods, so it is possible to see the skin layers better. Although the ability of PEG to increase the skin penetration of some compounds is known [23], the use of the hexagonal liquid crystalline phase nanodispersion resulted in greater PS skin penetration into deeper skin layers. This behavior can be assigned to the occlusive layer formed by water evaporation

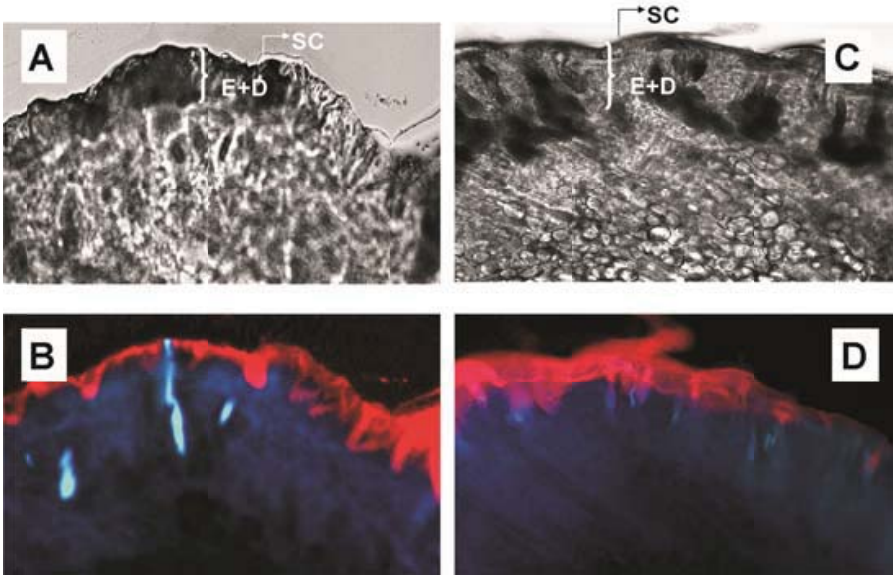

Fig. (6). Microscopic evaluation of the skin after *in vivo* penetration studies, as observed by fluorescent microscope operating with 395 and 440 nm band-pass excitation and emission filter, respectively. Pictures of the treated skin with control formulation containing PS, photographed without fluorescence light (**A**) and with fluorescence light (**B**). Pictures of skin treated with hexagonal nanodispersion containing PS photographed without fluorescence light (**C**) and with fluorescence light (**D**).

from nanodispersion, which facilitates the PS skin penetration, a crucial condition for the effectiveness of PDT. As previously observed by Lopes *et al.* [14] for cyclosporine A using fluorescence microscopy, in this work, the nanodispersion led to enhanced skin penetration of the PS.

CONCLUSIONS

The present work has demonstrated a formulation strategy to deliver topically a chlorin derivative to the skin for PDT purposes. A nanodispersed liquid crystalline phase containing chlorin was developed and revealed an hexagonal liquid crystalline structure, which has already proved to be advantageous for skin delivery of different drugs. Furthermore, the delivery system studied has important characteristics for use in the topical PDT of skin cancer, such as small particle size (less than 200 nm) combined to low cytotoxicity for normal skin fibroblasts cell line and improved PS uptake by deeper skin layers, where, in pathological conditions, neoplasic and non-neoplasic lesions take place.

CONFLICT OF INTEREST

The authors confirm that this article content has no conflicts of interest.

ACKNOWLEDGEMENTS

This work was supported by "Fundação de Amparo à Pesquisa do Estado de São Paulo" (FAPESP, Brazil, projects # 04/09465-7, # 08/06619-4 and # 09/00009-2) and "Conselho Nacional de Pesquisa" (CNPq, Brazil, projects # 482325/2007-0 and # 479275/2009-2). Thanks are also due to the CAPES (Brazil) /FCT (Portugal) for received funding under a collaborative protocol. R. Petrilli was the recipient of a CNPq fellowship (process # 109984/2007-2).

ABBREVIATIONS

PDT	=	Photodynamic therapy
SAXRD	=	Small angle X-ray diffraction
PS	=	Photosensitizing drug
OA	=	Oleic acid
MO	=	Monoolein
PEG	=	Polyethylene glycol
LOD	=	Limits of detection
LLOQ	=	Lower limit of quantification
Pdl	=	Polydispersity index
DLS	=	Light scattering method
a	=	Lattice parameter
FWHM	=	Full width at half maximum
SC	=	Stratum corneum
E+D	=	Epidermis plus dermis

REFERENCES

[1] Anand, S.; Ortel, B. J.; Pereira, S. P.; Hasan, T.; Maytin, E. V. Biomodulatory approaches to photodynamic therapy of solid tumors. *Cancer Lett.*, **2012**, *326*, 8-16.

[2] Robertson, C. A.; Evans, D. H.; Abrahamse, H. Photodynamic therapy (PDT): a short review on cellular mechanisms and cancer research applications for PDT. *J. Photochem. Photobiol. B*, **2009**, *96*, 1-8.

[3] Chen, J. X.; Wang, H. Y.; Li, C.; Han, K.; Zhang, X. Z.; Zhuo, R. Z. Construction of surfactant-like tetra-tail amphiphilic peptide with RGD ligand for encapsulation of porphyrin for photodynamic therapy. *Biomaterials*, **2011**, *32*, 1678-1684.

[4] Medina, W. S; Dos Santos, N. A.; Curti, C.; Tedesco, A. C.; Dos Santos, A. C. Effects of zinc phthalocyanine tetrasulfonate-based photodynamic therapy on rat brain isolates mitochondria. *Chem. Biol. Interact.*, **2009**, *179*, 402-406.

[5] Prokop, A. Davidson, J. M. Nanovehicular intracellular delivery systems. *J. Pharm. Sci.*, **2008**, *97*, 3518-3586.

[6] Nishiyama, N.; Nakagishi, Y.; Morimoto, Y.; Lai, P.S.; Miyazaki, K.; Urano, K.; Horie, S.; Kumagai, M.; Fukushima, S.; Cheng, Y.; Jang, W.D.; Kikuchi, M.; Kataoka, K. Enhancer photodynamic cancer treatment by supramolecular nanocarriers charged with dendrimer phtalocyanine. *J. Control. Release*, **2009**, *133*, 245-251.

[7] Pierre, M. B. R.; Tedesco, A. C.; Marchetti, J. M.; Bentley, M. V. L. B. Stratum corneum lipidis liposomes for the topical delivery of 5- aminolevulinic acid in photodynamic therapy of skin cancer: preparation and *in vitro* permeation study. *BMC Dermatol.*, **2001**, *1*, 1-6.

[8] Fang, Y. P.; Tsai, Y. H.; Wu, P. C.; Huang, Y. B. Comparison of 5-aminolevulinic acid-encapsulated liposome versus ethosome for skin delivery for photodynamic therapy. *Int. J. Pharm.*, **2008**, *356*, 144-152.

[9] Curic, N. D.; Gra¨fe, S.; Albrecht, V.; Fahr, A. Topical application of temoporfin-loaded invasomes for photodynamic therapy of subcutaneously implanted tumours in mice: A pilot study. *J. Photochem. Photobiol. B*, **2008**, *91*, 41-50.

[10] Primo, F. L.; Rodrigues, M. M. A.; Simioni, A. R.; Bentley, M. V. L. B.; Morais, P. C.; Tedesco, A. C. *In vitro* studies of cutaneous retention of magnetic nanoemulsion loaded with zinc phthalocyanine for synergic use in skin cancer treatment. *J. Magn. Magn. Mater.*, **2008**, *320*, 211-214.

[11] Singh, S. Phase transitions in liquid crystals. *Phys. Rep.*, **2000**, *324*, 107-269.

[12] Guo, C.; Wang, J.; Cao, F.; Lee, R.J.; Zhai, G. Lyotropic liquid crystal systems in drug delivery. *Drug Discov. Today*, **2010**, *15*, 1032-1040.

[13] Libster, D.; Ishai, P. B.; Aserin, A.; Shoham, G.; Garti, N. Molecular interactions in reverse hexagonal mesophase in the presence of Cyclosporin A. *Int. J. Pharm*., **2009**, *367*, 115-126.

[14] Lopes, L. B.; Ferreira, D. A.; Paula, D.; Garcia, N. T. J.; Thomazini, J. A.; Fantini, M. C. A.; Bentley, M. V. L. B. Reverse hexagonal phase nanodispersion of monoolein and oleic acid for topical delivery of peptides: *in vitro* and *in vivo* skin penetration of Cyclosporin A. *Pharm. Res.*, **2006**, *23*, 1332-1342.

[15] Lopes, L. B.; Speretta, F. F. F.; Bentley, M. V. L. B. Enhancement of skin penetration of vitamin K using monoolein-based liquid crystalline systems. *Eur. J. Pharm. Sci.*, **2007**, *32*, 209-215.

[16] Carr, M. G.; Corish, J.; Corrigan, O. I. Drug delivery from a liquid crystalline base across Visking and human stratum corneum. *Int. J. Pharm.*, **1997**, *157*, 35-42.

[17] Lopes, L. B.; Lopes, J. L. C.; Oliveira, D. C. R.; Thomazini, J. A.; Garcia, M. T. J.; Fantini, M. C. A.; Collett, J. H.; Bentley, M. V. L. B. Liquid crystalline phases of monoolein and water for topical delivery of cyclosporine A: characterization and study of *in vitro* and *vivo* delivery. *Eur. J. Pharm. Biopharm*., **2006**, *63*, 146-155.

[18] Vicentini, F. T. M. C.; Depieri, L. V.; Polizello, A. C. M.; Del Ciampo, J. O.; Spadaro, A. C.; Fantini, M. C. A.; Bentley, M. V. L. B. Liquid crystalline phase nanodispersions enable skin delivery of siRNA. *Eur. J. Pharm. Biopharm*., **2013**, *83*, 16-24.

[19] de Oliveira, K. T.; Silva, A. M. S.; Tomé, A. C.; Neves, M. G. P. M. S.; Neri, C. R.; Garcia, V. S.; Serra, O. A.; Iamamoto, Y.; Cavaleiro, J. A. S. Synthesis of new amphiphilic chlorin derivatives from protoporphyrin-IX dimethyl ester. *Tetrahedron*, **2008**, *64*, 8709-8715.

[20] Mojzisova, H.; Bonneau, S.; Bizet, C. V.; Brault, D. The pH-dependent distribution of the photosensitizer chorin e6 among plasma proteins and membranes: a physico-chemical approach. *Biochim. Biophys. Acta*, **2007**, *1768*, 366-374.

[21] Praça, F. S. G; Medina, W. S. G; Petrilli, R.; Bentley, M.V.L.B. Liquid crystal nanodispersions enable the cutaneous delivery of photosensitizer for topical PDT: fluorescence microscopy study of skin penetration. *Curr. Nanosci*., **2012**, 8, 1-8.

[22] Fisichella, M.; Dabboue, H.; Bhattacharyya, S.; Saboungi, M. L.; Salvetat, J. P.; Hevor, T.; Guerin, M. Mesoporous silica nanoparticles enhance MTT formazan exocytosis in HeLa cells and astrocytes. *Toxicol. In Vitro*, **2009**, *23*, 697-703.

Received: November 20, 2012 Revised: March 13, 2013 Accepted: April 25, 2013

[23] Cevc, G.; Richardsen, H. Lipid vesicles and membrane fusion. *Adv. Drug Deliv. Rev.*, **1999**, *38*, 207-232.

[24] de Rosa, F. S.; Tedesco, A. C.; Lopez, R. F. V.; Pierre, M. B. R.; Lange, N.; Rotta, J. C. G.; Marchetti, J. M.; Bentley, M. V. L. B. *In vitro* skin permeation and retention of 5-aminolevulinic acid ester derivatives for photodynamic therapy. *J. Control. Release*, **2003**, *89*, 261-269.

[25] W¨orle, G.; Drechsler, M.; Koch, M. H. J.; Siekmann, B.; Westesen, K.; Bunjes, V. Influence of composition and preparation parameters on the properties of aqueous monoolein dispersions. *Int. J. Pharm.*, **2007**, *329*, 150-157.

[26] Nakano, M.; Sugita, A.; Matsuoka, H.; Handa, T. Small-Angle X-ray Scattering and 13C NMR Investigation on the Internal Structure of "Cubosomes". *Langmuir*, **2001**, *17*, 3917-3922.

[27] Helledi, L. S.; Schubert, L. Release Kinetics of Acyclovir from a Suspension of Acyclovir Incorporated in a cubic phase delivery system. *Drug Dev. Ind. Pharm.*, **2001**, *27*, 1073-1081.

[28] Rossetti, F. C.; Fantini, M. C. A.; Carollo, A. R. H.; Tedesco, A. C.; Bentley, M. V. L. B. Analysis of Liquid Crystalline Nanoparticles by Small Angle X-Ray Diffraction: Evaluation of Drug and Pharmaceutical Additives Influence on the Internal Structure. *J. Pharm. Sci.*, **2011**, *100*, 2849-2857.

[29] Nakano, M.; Teshigawara, T.; Sugita, A.; Leesajakul, W.; Taniguchi, A.; Kamo, T.; Matsuoka, H.; Handa, T. Dispersions of Liquid Crystalline Phases of the Monoolein/ Oleic Acid/Pluronic F127 System. *Langmuir*, **2002**, *18*, 9283-9288.

[30] Vemuri, S.; Rhodes, C.T. Encapsulation of a water soluble drug in a liposome preparation: removal of free drug by washing. *Drug Dev. Ind. Pharm*., **1995**, *21*, 1329-1338.

[31] Lopes, L. B.; Vandewall, H.; Li, H. T.; Venugopal, V.; Li, H. K.; Naydin, S.; Hosmer, J.; Levendusky, M.; Zheng, H.; Bentley, M. V. L. B.; Levin, R.; Hass, M. A. Topical Delivery of Lycopene Using Microemulsions: Enhanced Skin Penetration and Tissue Antioxidant Activity. *J. Pharm. Sci*., **2010**, *99*, 1346-1357.

[32] OECD. Guideline for the testing of chemicals No. 428. Skin Absorption: *In vitro* Method, Paris, France, **2004**.

[33] Busch, P.; Müller, R.; Pitterman, W. Uses and limitations of the porcine skin model in cosmetic research. *Parfümerie Kosmetik ,* **1996**, *77*, 20-27.

[34] Cevc, G. Lipid vesicles and other colloids as drug carriers on the skin. *Adv. Drug Deliv. Rev*. **2004**, *56*, 675-711.

[35] Esposito, E.; Cortesi, R.; Drechsler, M.; Paccamiccio, L.; Mariani, P.; Contado, C.; Stellin, E.; Menegatti, E.; Bonina, F.;, Puglia, C. Cubosome Dispersions as Delivery Systems for Percutaneous Administration of Indomethacin. *Pharm. Res.*, **2005**, *22*, 2163–2173.

[36] Foldvari, M.; Baca-Estrada, M.E.; He, Z.; Hu, J.; Attah-Poku, S.; King, M. Dermal and transdermal delivery of protein pharmaceuticals: lipid-based delivery systems for interferon α. *Biotechnol. Appl. Biochem.*, **1999**, *30*, 129-137.